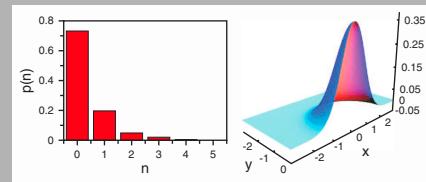


# LASER PHYSICS LETTERS

www.lphys.org

**Abstract:** We report the generation and the tomographic analysis of novel quantum states of light generated by the controlled addition and subtraction of single photons to and from a classical and fully incoherent thermal light field. Time-domain quantum tomography is used to thoroughly investigate the character of the resulting states. Several different criteria are employed to test and quantify nonclassicality of photon-added thermal states, while the peculiar features concerning the mean photon number of photon-subtracted thermal states are clearly observed.



Experimental photon number probabilities and Wigner function for a thermal state

© 2008 by Astro Ltd.  
Published exclusively by WILEY-VCH Verlag GmbH & Co. KGaA

## Manipulating thermal light states by the controlled addition and subtraction of single photons

V. Parigi,<sup>1,2</sup> A. Zavatta,<sup>2,3</sup> and M. Bellini<sup>1,3</sup>

<sup>1</sup> LENS, Via Nello Carrara 1, 50019 Sesto Fiorentino, Florence, Italy

<sup>2</sup> Department of Physics, University of Florence, 50019 Sesto Fiorentino, Florence, Italy

<sup>3</sup> Istituto Nazionale di Ottica Applicata - CNR, 6, L. go E. Fermi, 50125, Florence, Italy

Received: 20 November 2007, Accepted: 24 November 2007

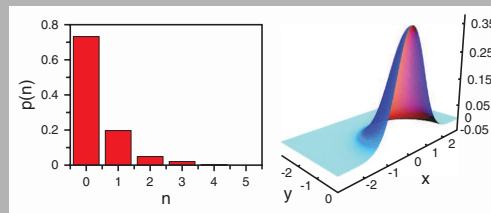
Published online: 29 November 2007

Laser Phys. Lett. **5**, No. 3, 246–251 (2008) / DOI 10.1002/lapl.200710119

 WILEY

REPRINT

**Abstract:** We report the generation and the tomographic analysis of novel quantum states of light generated by the controlled addition and subtraction of single photons to and from a classical and fully incoherent thermal light field. Time-domain quantum tomography is used to thoroughly investigate the character of the resulting states. Several different criteria are employed to test and quantify nonclassicality of photon-added thermal states, while the peculiar features concerning the mean photon number of photon-subtracted thermal states are clearly observed.



Experimental photon number probabilities and Wigner function for a thermal state

© 2008 by Astro Ltd.

Published exclusively by WILEY-VCH Verlag GmbH & Co. KGaA

## Manipulating thermal light states by the controlled addition and subtraction of single photons

V. Parigi,<sup>1,2</sup> A. Zavatta,<sup>2,3</sup> and M. Bellini<sup>1,3,\*</sup>

<sup>1</sup> LENS, Via Nello Carrara 1, 50019 Sesto Fiorentino, Florence, Italy

<sup>2</sup> Department of Physics, University of Florence, 50019 Sesto Fiorentino, Florence, Italy

<sup>3</sup> Istituto Nazionale di Ottica Applicata - CNR, 6, L. go E. Fermi, 50125, Florence, Italy

Received: 20 November 2007, Accepted: 24 November 2007

Published online: 29 November 2007

**Key words:** nonclassical states; single photons; homodyne tomography

**PACS:** 03.65.Wj, 42.50.Dv

### 1. Introduction

The emergent field of quantum technology holds promise of a revolution in the way information is processed, communicated and stored. In particular, photonic states and devices are currently viewed as the most promising candidates to transport and manipulate quantum information. The ability to reliably generate and manipulate states of light with nonclassical features is thus one of the keys towards the successful implementation of these future technologies. The interaction of laser light with nonlinear crystals, and the subsequent parametric generation of pairs of photons characterized by a common, non-factorizable wavefunction, is at the basis of most of the currently proposed schemes for quantum computation and communication.

While discrete variable systems were initially considered for the theoretical and experimental investigations of such protocols, the use of infinite-dimensionality, or continuous variable (CV), systems has lately been considered

as a very natural and rich extension [1]. Although Gaussian CV states are in principle sufficient for a wide range of proposed protocol implementations, some more elaborate schemes require the use of non-Gaussian resources. In particular, non-Gaussian states and operations are now viewed as a fundamental requirement for CV quantum technologies because, besides enhancing some existing protocols [2–5], they are also able to perform important communication and computation tasks (like entanglement distillation) which are impossible with Gaussian states and operations only [6, 7].

However, the generation of non-Gaussian states and the implementation of non-Gaussian operations for CV protocols have been limited to very few cases, so far. Only recently, some nonclassical non-Gaussian states and de-Gaussification procedures have become experimentally accessible [8–12], but these laboratory realizations have not kept the pace of the huge and increasing number of theoretical proposals.

\* Corresponding author: e-mail: bellini@inoa.it



type-I BBO crystal which generates spontaneous parametric down-conversion (SPDC) at the same wavelength of the laser source. Pairs of SPDC photons are emitted in two distinct spatial channels called signal and idler. Along the idler channel the photons are strongly filtered in the spectral and spatial domain by means of etalon cavities and by a single-mode fiber (F) which is directly connected to a single-photon-counting module (see Fig. 1); indeed the remotely-prepared signal state will only approach a pure state if the filter transmission function is much narrower than the momentum and spectral widths of the pump beam generating the SPDC pair (further details are given in [17, 18]).

Whenever a single photon is detected in the idler channel, an homodyne measurement is performed on the correlated spatiotemporal mode of the signal channel. When no seed field is injected in the SPDC crystal, conditional single-photon Fock states are generated from spontaneous emission in the signal channel [19, 17]. By injecting a thermal state into the SPDC input signal mode, an idler trigger event conditions the stimulated production of a single-photon-excited thermal state in the output signal mode, as recently demonstrated by our group also in the case of a coherent state seed [9, 18].

## 2.2. Single photon subtraction

Photon subtraction by the operator  $\hat{a}$  is simply implemented by blocking the SPDC pump and inserting a high-transmissivity BS (formed by a combination of half-wave plate ( $\lambda/2$ ) and polarizing beam splitter (PBS)) in the path of the signal mode containing the thermal state (see Fig. 2). In this case the trigger signal for homodyne measurements is obtained from a click in the on/off detector placed in the path of the reflected photons [8], provided that great care is used to make sure that photons are subtracted from exactly the same spatiotemporal mode as the one defined by the local oscillator.

## 2.3. Pulsed homodyne detection

The signal field is mixed with a strong local oscillator (LO, an attenuated portion of the main laser source) on a 50% beam-splitter (BS-H) (see Fig. 1 and Fig. 2). The pulses at the BS outputs are detected by two photodiodes (Hamamatsu S3883, with active area  $1.7 \text{ mm}^2$ ) connected to the positive and negative inputs of a wide-bandwidth amplifier which provides the difference (homodyne) signal between the two photocurrents on a pulse-to-pulse basis [20, 21]. The detector shows a linear response up to LO powers of about 9 mW, and with a signal-to-noise ratio of about 12 dB when the device is operated at the optimum LO power of 8 mW. Whenever a trigger pulse is received, an homodyne measurement is performed on the selected spatiotemporal mode of the signal channel by storing the corresponding electrical signal (proportional to the quadrature

operator value) on a digital scope. In order to decrease the effect of the dark counts in the single-photon trigger detector, a strict coincidence with the signal coming from the laser pulse train is used as the trigger for the acquisition of the homodyne signal. Although this slightly reduces the trigger count rate, it is effective in increasing the ratio of “true” to “false” trigger events to more than 99%. Being the studied fields completely phase invariant, we choose to acquire a total of about  $10^5$  quadrature measurements for each investigated state while leaving the LO phase unlocked.

## 3. Data analysis and discussion

If the parametric gain of the SPDC crystal and the reflectivity of the subtracting BS are low enough, the two above operations are a good approximation of the ideal processes of photon addition and subtraction by the operators  $\hat{a}^\dagger$  and  $\hat{a}$  acting on the signal mode. Both conditions are well satisfied in our experiment (with a BS reflectivity of about 1% and a parametric gain of 0.01) and we can thus use a simple description of the final states as:

$$\hat{\rho}_{add} \propto \hat{a}_s^\dagger \hat{\rho} \hat{a}_s = \frac{1}{\bar{n}(\bar{n}+1)} \sum_{n=0}^{\infty} \left( \frac{\bar{n}}{1+\bar{n}} \right)^n n|n\rangle\langle n|,$$

$$\hat{\rho}_{sub} \propto \hat{a}_s \hat{\rho} \hat{a}_s^\dagger = \frac{1}{(\bar{n}+1)^2} \sum_{n=0}^{\infty} \left( \frac{\bar{n}}{1+\bar{n}} \right)^n (1+n)|n\rangle\langle n|,$$

where  $\hat{\rho}$  is the density matrix of the initial thermal state with  $\bar{n}$  corresponding to its mean number of photons. It is evident that the initial thermal distributions are modulated by these operations and, in the case of photon addition, the completely classical and incoherent initial state is transformed into a purely quantum state as clearly testified by the lack of the vacuum contribution [22].

### 3.1. Quantum state reconstruction

We have performed the reconstruction of the diagonal density matrix elements using the maximum likelihood estimation [23]. This method gives the density matrix that most likely represents the measured homodyne data. Firstly, we build the likelihood function contracted for a density matrix truncated to 15 diagonal elements (with the constraints of Hermiticity, positivity, and normalization), then the function is maximized by an iterative procedure [24, 25] and the errors on the reconstructed density matrix elements are evaluated using the Fisher information [25]. Note that no correction for the finite detection efficiency is introduced in the reconstruction procedure. Finally we use the retrieved density matrix elements for a straightforward calculation of the corresponding Wigner functions [18]. Although the finite experimental efficiency in the preparation and detection of the states results in a mixture with

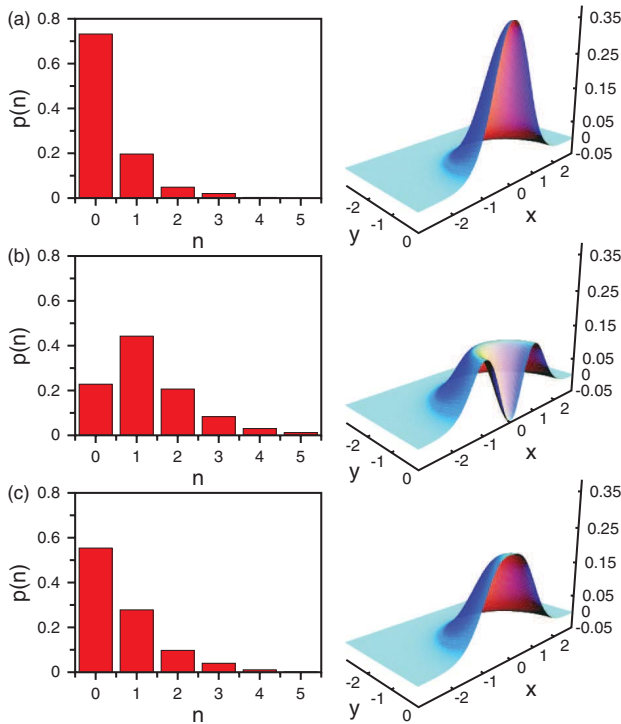


**Figure 3** (online color at [www.lphys.org](http://www.lphys.org)) Experimentally reconstructed diagonal density matrix elements (photon number probabilities) and Wigner functions for (a) thermal state, (b) photon-added, and (c) photon-subtracted thermal states

vacuum which smoothens the distributions, the nonclassicality of the photon-added state is apparent from the negativity of its Wigner function, while the de-Gaussification of the photon-subtracted state is also clearly observable as a flattening of its top portion (see Fig. 3).

### 3.2. Nonclassicality criteria

The photon-added thermal state is expected to show a nonclassical character independent of the mean number of photons in the seed thermal state. In the case of finite efficiency, the expression for the Wigner function results:

$$W_{\eta}(\alpha) = \frac{2}{\pi} \frac{1 + 2\eta[\bar{n} + 2(1 + \bar{n})|\alpha|^2 - 2\bar{n}\eta - 1]}{(1 + 2\bar{n}\eta)^3} \exp\left(\frac{-2|\alpha|^2}{1 + 2\bar{n}\eta}\right), \quad (1)$$

where  $\alpha = x + iy$  and the nonclassical features of the state are clearly seen to get weaker for large  $\bar{n}$ , as the limited efficiency ( $\eta < 1$ ) has the effect of progressively hiding them among unwanted vacuum components. Indeed, the measured negativity of the Wigner function at the origin rapidly gets smaller as the mean photon number of the input thermal state is increased. With the current level

of efficiency and reconstruction accuracy we are able to prove the nonclassicality of all the generated states up to  $\bar{n} = 1.15$ . It should be noted that, even for a single-photon Fock state, the Wigner function loses its negativity for efficiencies lower than 50%, so that surpassing this experimental threshold is an essential requisite in order to use this nonclassicality criterion.

The nonclassical character of the measured photon-added thermal states can be verified also using different criteria. The first one has been recently proposed by Richter and Vogel [26] and is based on the characteristic function  $G(k, \theta) = \langle \exp[ik\hat{x}(\theta)] \rangle$  of the quadratures (i.e., the Fourier transform of the quadrature distribution), where  $\hat{x}(\theta) = [\hat{a} \exp(-i\theta) + \hat{a}^{\dagger} \exp(i\theta)]/2$  is the phase-dependent quadrature operator. At the first-order, the criterion defines a phase-independent state as nonclassical if there is a value of  $k$  such that the state characteristic function is larger than the vacuum one. In other words, the evidence of structures narrower than those associated to vacuum in the quadrature distribution is a sufficient condition to define a nonclassical state [27]. This is just a sufficient condition and it has to be extended in the case of particular quantum states. However, as higher orders are investigated, the increasing sensitivity to experimental and statistical noise may soon become unmanageable. We found that the first-order criterion only works for the two lowest values of  $\bar{n}$  and that the extension to the second order, just barely shows nonclassicality at large values of  $k$  for  $\bar{n}$  up to 0.53. At higher equivalent temperatures, no sign of nonclassical behavior is experimentally evident with this approach, although the Wigner function of the corresponding states still clearly exhibits a measurable negativity.

The tomographic reconstruction of the state can also be exploited to test alternative criteria: for example by reconstructing the photon-number distribution  $\rho_n = \langle n | \hat{\rho}_{meas} | n \rangle$  and then looking for strong modulations in neighboring photon probabilities by the following relationship [28,29]

$$B(n) \equiv (n + 2)\rho_n\rho_{n+2} - (n + 1)\rho_{n+1}^2 < 0, \quad (2)$$

introduced by Klyshko in 1996, which is known to hold for nonclassical states. In the ideal situation of unit efficiency single-photon-added thermal states should always give  $B(0) < 0$  due to the absence of the vacuum term  $\rho_0$ , in agreement with [22]. In this case, differently from the Wigner function approach, the nonclassicality can be proved even for experimental efficiencies much lower than 50%, as far as the mean photon number of the thermal state is not too high (see Fig. 4b).

Finally, we evaluate the nonclassicality of the states by quantifying their entanglement potential (EP) as recently proposed by Asboth et al. [30]. This measurement is based on the fact that, when a nonclassical state is mixed with vacuum on a 50-50 beam splitter, some amount of entanglement (depending on the nonclassicality of the input state) appears between the BS outputs. No entanglement can be produced by a classical initial state. For a given

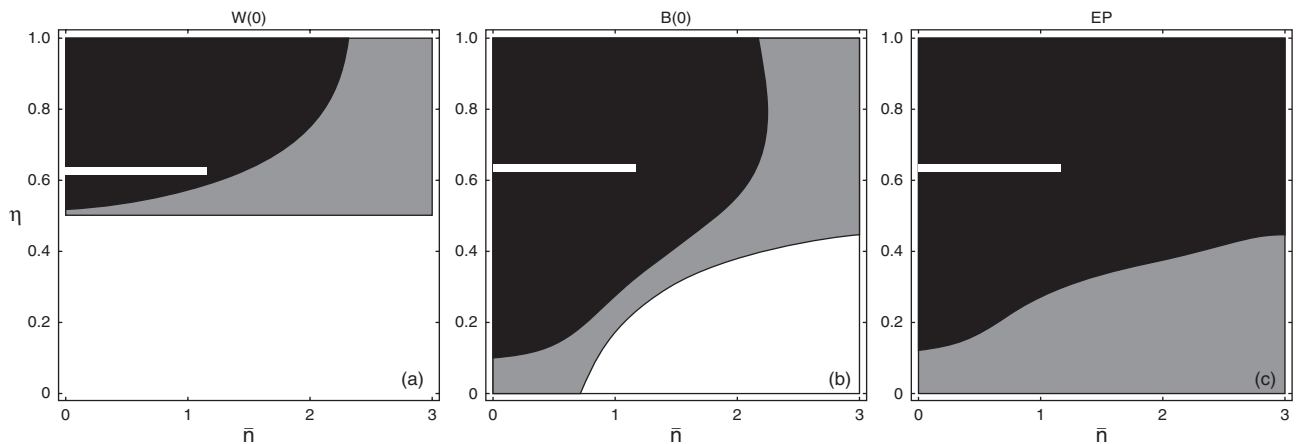


**Figure 4** Calculated regions of nonclassical behavior of single-photon-added thermal states as a function of  $\bar{n}$  and  $\eta$  according to: (a) the negativity of the Wigner function at the origin  $W(0)$ ; (b) the Klyshko criterion  $B(0)$ ; (c) the entanglement potential EP. White areas indicate classical behavior; grey areas indicate where a potentially nonclassical character is not measurable due to experimental reconstruction noise (estimated as the average error on the experimentally reconstructed parameters); black areas indicate regions where the nonclassical character is measurable given the current statistical uncertainties. The white stripe area in each plot corresponds to the range of parameters investigated in the present experiment

single-mode density operator, one can calculate the entanglement of the bipartite state at the BS outputs by computing its logarithmic negativity. The entanglement potential derived from the reconstructed density matrices of the single-photon added thermal states is definitely greater than zero for all the detected states, thus confirming that they are indeed nonclassical, in agreement with the findings obtained by the measurement of  $B(0)$  and  $W(0)$ . We have calculated the indicators  $W(0)$ ,  $B(0)$ , and EP from a model state including the current experimental inefficiency. The results are shown in Fig. 4 together with the range of parameters investigated here (denoted by the white stripe): the contour plots define the regions of parameters where the detected state is classical (white areas), where it would result nonclassical if the reconstruction errors coming from statistical noise could be neglected (grey areas) and, finally, where it is definitely nonclassical even with the current level of noise (black areas).

From such plots it is evident that all the three tomographic approaches to test nonclassicality are able to experimentally prove it for all the generated states (i.e., single-photon-added thermal states with an average number of photons in the seed thermal state up to  $\bar{n} = 1.15$ ) for a global experimental efficiency of  $\eta = 0.62$ . However, as already noted, the Wigner function negativity only works for sufficiently high efficiencies, while both  $B(0)$  and EP are able to detect nonclassical behavior even for  $\eta < 50\%$ . In particular, the entanglement potential is clearly seen to be the most powerful criterion, at least for these particular states, and to allow for an experimental proof of nonclassicality for all combinations of  $\bar{n}$  and  $\eta$ , as long as reconstruction errors can be neglected. Also considering the current experimental parameters, EP should show the

quantum character of single-photon-added thermal states even for  $\bar{n} > 3$ , thus demonstrating its higher immunity to noise [11].

### 3.3. Mean photon numbers

When applying the annihilation operator  $\hat{a}$  to an arbitrary light state, some counterintuitive effects can be obtained in the mean number of photons of the output state. As already shown in the context of photodetection theory [31, 32], one can easily find that the average number of photons in the “photon-subtracted” state,  $\bar{n}_{sub}$ , is related to the initial one,  $\bar{n}$  as:

$$\bar{n}_{sub} = \bar{n} - 1 + F, \quad (3)$$

where  $F$  is the Fano factor of the initial state, simply given by the ratio between the photon number variance and the mean, which is greater, equal to, or less than unity for Super-Poissonian, Poissonian, or Sub-Poissonian initial states, respectively. So, depending on the character of the initial state, the mean photon number in the final state can be less than, equal to, or even larger than before “photon subtraction”. Furthermore, unless the initial state is a coherent one, the whole statistics of the field is changed by this process. The reason for this behavior stems from the proportionality factor  $\sqrt{n}$  appearing in the expression for the action of the annihilation operator on a Fock state  $|n\rangle$  which, besides shifting the photon distribution to the left, favors the action of the operator upon the higher excited states, so that it may effectively increase the relative weight of higher-energy components in the final state. Indeed, the successful event of particle subtraction by  $\hat{a}$

preferentially selects the subset of states having a larger probability of giving a particle away, i.e., those containing a larger number of photons. It should be stressed that this is not a quantum effect, since a similar increase in the mean photon number may also be expected in a classical case if particle subtraction is performed in a probabilistic way. After subtracting a photon from a thermal field, the average photon number grows from  $\bar{n}$  to  $2\bar{n}$ . On the other hand, the operation of photon addition increases the mean photon number of the thermal field even further to  $2\bar{n} + 1$ . Our experimental results, once corrected for the limited detection efficiency, confirm such predictions: by subtracting a photon from a thermal state with a mean photon number of 0.57, we obtain  $\bar{n}_{sub} \approx 1.1$ , while adding a photon to the same state results in  $\bar{n}_{add} \approx 2.0$  (see Fig. 3).

#### 4. Conclusions

We have demonstrated the generation of novel light states by adding and subtracting single photons to/from a completely classical thermal field. Then we have used quantum homodyne tomography to completely characterize the resulting states. The single-photon added thermal states have shown a continuously adjustable degree of quantumness which makes them the ideal test bed for assessing the performances of current experimental approaches to quantify nonclassicality. On the other hand, the subtraction of a single photon from a thermal state has resulted in its clear de-Gaussification. Furthermore, the intriguing increase of the mean photon number in a photon-subtracted state has been observed and discussed. Finally, the successful experimental implementation of the basic quantum operators of photon addition and subtraction and of their sequences [12] may constitute a fundamental step in the realization of a completely customizable quantum light state for future quantum technologies.

*Acknowledgements* This work has been partially supported by Ente Cassa di Risparmio di Firenze and MIUR under the PRIN2005 initiative.

#### References

- [1] S.L. Braunstein and P. van Loock, *Rev. Mod. Phys.* **77**, 513 (2005).
- [2] T. Opatrný, G. Kurizki, and D.-G. Welsch, *Phys. Rev. A* **61**, 032302 (2000).
- [3] P.T. Cochrane, T.C. Ralph, and G.J. Milburn, *Phys. Rev. A* **65**, 062306 (2002).
- [4] S. Olivares, M.G.A. Paris, and R. Bonifacio, *Phys. Rev. A* **67**, 032314 (2003).
- [5] N.J. Cerf, O. Krüger, P. Navez, R.F. Werner, and M.M. Wolf, *Phys. Rev. Lett.* **95**, 070501 (2005).
- [6] J. Eisert, S. Scheel, and M.B. Plenio, *Phys. Rev. Lett.* **89**, 137903 (2002).
- [7] G. Giedke and J.I. Cirac, *Phys. Rev. A* **66**, 032316 (2002).
- [8] J. Wenger, R. Tualle-Brouri, and P. Grangier, *Phys. Rev. Lett.* **92**, 153601 (2004).
- [9] A. Zavatta, S. Viciani, and M. Bellini, *Science* **306**, 660 (2004).
- [10] A. Ourjoumtsev, R. Tualle-Brouri, J. Laurat, and P. Grangier, *Science* **312**, 83 (2006).
- [11] A. Zavatta, V. Parigi, and M. Bellini, *Phys. Rev. A* **75**, 052106 (2007).
- [12] V. Parigi, A. Zavatta, M. Kim, and M. Bellini, *Science* **317**, 1890 (2007).
- [13] R.J. Glauber, *Phys. Rev.* **131**, 2766 (1963).
- [14] E.C.G. Sudarshan, *Phys. Rev. Lett.* **10**, 277 (1963).
- [15] M.S. Kim, E. Park, P.L. Knight, and H. Jeong, *Phys. Rev. A* **71**, 043805 (2005).
- [16] F.T. Arecchi, *Phys. Rev. Lett.* **15**, 912 (1965).
- [17] A. Zavatta, S. Viciani, and M. Bellini, *Phys. Rev. A* **70**, 053821 (2004).
- [18] A. Zavatta, S. Viciani, and M. Bellini, *Phys. Rev. A* **72**, 023820 (2005).
- [19] A.I. Lvovsky, H. Hansen, T. Aichele, O. Benson, J. Mlynek, and S. Schiller, *Phys. Rev. Lett.* **87**, 050402 (2001).
- [20] A. Zavatta, M. Bellini, P.L. Ramazza, F. Marin, and F.T. Arecchi, *J. Opt. Soc. Am. B* **19**, 1189 (2002).
- [21] A. Zavatta, S. Viciani, and M. Bellini, *Laser Phys. Lett.* **3**, 3 (2006).
- [22] C.T. Lee, *Phys. Rev. A* **52**, 3374 (1995).
- [23] K. Banaszek, G.M. D'Ariano, M.G.A. Paris, and M.F. Sacchi, *Phys. Rev. A* **61**, 010304 (1999).
- [24] A.I. Lvovsky, *J. Opt. B* **6**, S556 (2004).
- [25] Z. Hradil, D. Mogilevtsev, and J. Řeháček, *Phys. Rev. Lett.* **96**, 230401 (2006).
- [26] W. Vogel, *Phys. Rev. Lett.* **84**, 1849 (2000).
- [27] A.I. Lvovsky and J.H. Shapiro, *Phys. Rev. A* **65**, 033830 (2002).
- [28] D.N. Klyshko, *Phys. Lett. A* **213**, 7 (1996).
- [29] G.M. D'Ariano, M.F. Sacchi, and P. Kumar, *Phys. Rev. A* **59**, 826 (1999).
- [30] J.K. Asbóth, J. Calsamiglia, and H. Ritsch, *Phys. Rev. Lett.* **94**, 173602 (2005).
- [31] M. Ueda, N. Imoto, and T. Ogawa, *Phys. Rev. A* **41**, 3891 (1990).
- [32] S.S. Mizrahi and V.V. Dodonov, *J. Phys. A* **35**, 8847 (2002).